Journal of Soils and Sediments
https://doi.org/10.1007/s11368-019-02539-5

SEDIMENTS, SEC 4 • SEDIMENT-ECOLOGY INTERACTIONS • RESEARCH ARTICLE

Effects of cyanobacterial accumulation and decomposition on the microenvironment in water and sediment

Weizhen Zhang[1] · Peng Gu[1] · Wenjie Zhu[2] · Chaosen Jing[1] · Jian He[1] · Xiaoying Yang[1] · Liang Zhou[3] · Zheng Zheng[1]

Received: 7 September 2019 / Accepted: 2 December 2019

Abstract

Purpose Cyanobacterial blooms pose a serious threat to aquatic environmental health and have emerged as a primary issue in the recovery of eutrophic lakes. In order to comprehensively establish the effects of cyanobacterial blooms on nutrients in the aquatic environment, nutrient migration and transformation were studied in freshwater and sediments during cyanobacterial bloom decomposition.

Materials and methods Cyanobacteria and sediments were collected from Zhushan Bay, in Taihu Lake, and the process of cyanobacterial decomposition was simulated in the laboratory. The focus of this research was to assess the effects of cyanobacterial decomposition on physicochemical parameters and nutrient concentrations in water, the vertical distribution of nutrients in sediments. We also determined the moisture content (ΔC_w) and organic matter content (ΔOM) in surface sediments. Correlations were assessed between cyanobacterial decomposition and nutrient concentrations in water, with ΔC_w and ΔOM in surface sediments simultaneously analyzed.

Results and discussion In the water column, electric conductivity (Ec) was found to significantly increase, while dissolved oxygen (DO) and oxidation reduction potential (ORP) rapidly reduced. In addition, pH initially decreased and then increased, while ultraviolet light (UV_{254}) exhibited an opposite trend, which was related to the release and degradation of organic matter during the decomposition of cyanobacteria. Other nutrient concentrations were found to increase gradually with time, with the exception of nitrate nitrogen (NO_3^-–N), indicating that nutrients undergo temporal transitions between forms during cyanobacterial decomposition. Cyanobacterial decomposition causes ΔOM and ΔC_w to increase in surface sediment layers, affecting the vertical distribution of nutrient species in the sediment. The water-sediment interface nutrient flux intensity was ranked in the order total nitrogen (TN) > ammonia nitrogen (NH_4^+–N) > NO_3^-–N > total phosphorus (TP), which was related to the settlement of cyanobacterial debris during cyanobacterial decomposition. Good binomial relationships ($R^2 > 0.90$, $p < 0.05$) were found between cyanobacterial density and nutrient concentrations in the waterbody, as well as between cyanobacterial density and ΔOM or ΔC_w in the surface sediment.

Conclusions Cyanobacterial decomposition affected various water quality parameters, leading to nutrient migration and transformation in the water-sediment interface, providing nutrients to drive cyanobacterial bloom development.

Keywords Cyanobacterial bloom · Decomposition · Nutrients · Migration · Transformation

1 Introduction

Aquatic eutrophication results in the formation of harmful algal blooms (HABs), which pose a serious threat to water ecosystems, drinking water supplies, and human health worldwide (Ding et al. 2016; Han et al. 2018). In particular, cyanobacterial decomposition results in black-odorous waterbodies, deteriorating ecosystems, and serious damage to the health of lake ecosystems and water resources (Hoegh-Guldberg et al. 2009). The accumulation of cyanobacteria in water bodies can cause damage to aquatic

Responsible editor: Shiming Ding

✉ Zheng Zheng
zzhenghj@fudan.edu.cn

[1] Department of Environmental Science and Engineering, Fudan University, Shanghai 200438, China

[2] WuXi NextCODE, Shanghai 200131, China

[3] Nanjing Perennial Root Flowers Botanical Garden, Nanjing 210017, China

Published online: 03 April 2020

ecosystems, due to the release of cyanobacterial toxins, nutrients, and debris during lysis, which accumulates on the surface of sediments. This sedimentation process changes the nutritional status of sediments, causing surface sediments to act as both a nutrients source and sink (Papadimitriou et al. 2018). This in turn can lead to prolonged eutrophication (Bjerring et al. 2013) and the continued occurrence of cyanobacterial blooms (Yang et al. 2017). For example, it has been reported that total phosphorus (TP) released from sediments in Lake Dianchi (the largest lake in Southwestern China) could maintain the current TP water levels for 63 years (Hu et al. 2007). The accumulation of cyanobacteria and release of nutrients such as phosphorus and nitrogen has become a major cause of water quality deterioration (House and Denison 2002).

Many previous studies have shown that in many shallow lake environments, even if exogenous nutrient salts are controlled, cyanobacterial blooms continue to develop (Sahlsten and Sörensson 1989; Graham et al. 2010; Su et al. 2017). In some waters, the accumulation of cyanobacteria can reach several centimeters or even tens of centimeters (Qinglong et al. 2008). The decomposition of cyanobacteria consumes a large amount of dissolved oxygen in the water. In addition, a large amount of soluble nutrients are released into the water during decomposition, such as nitrogen and phosphorus, thereby changing the normal nutrient cycling patterns and increasing the nutrient load in the water (Beversdorf et al. 2017; Yan et al. 2017). Chen et al. (2018a, b, c) showed that the dissolved phosphorus released by cyanobacteria can account for 53% of the total phosphorus content of waterbodies. Furthermore, the decomposition rate of cyanobacterial debris was faster (0.072~0.271 day^{-1}), which leads to the rapid release of nutrients (Chen et al. 2018a, b, c). The process of nutrient release during cyanobacterial decomposition was affected by the degree of cyanobacteria aggregation, and the concentration of released nutrients increased with higher cyanobacterial bloom densities (Bianchi 2000; Ding et al. 2018). Paytan et al. (2016) showed that the accumulation and decomposition of cyanobacterial led to the release of nutrients from sediment interstitial water, which aggravated the nutrient loading in overlying water and supported the recurrence of cyanobacterial blooms. Kim and Kim (2013) found that the decomposition of cyanobacterial led to a rapid increase in nutrient concentrations in the water. Moreover, nutrient release was positively correlated with cyanobacterial concentrations (Nikolai and Dzialowski 2014).

Lake Taihu is the third largest freshwater lake in China, located in the Southeastern region of the Yangtze River Delta in the Chinese coastal plain, with an area of 2338 km^2, a catchment area of 36,500 km^2, and a volume of 4.4 billion m^3 (Qin et al. 2010). The annual input to Lake Taihu is about 57×10^8 m^3, with a water retention time of approximately 284 days (Duan et al. 2012). Lake Taihu exhibits two ecologically distinct regions, with the Northwestern region characterized by high water turbidity and frequent cyanobacteria bloom occurrence between late spring and early fall (Ye et al. 2010; Xu et al. 2013). In contrast, the eastern region of the lake is characterized by clear water with numerous surface and submersed macrophytes (Chen et al. 2018a, b, c). The locations and movements of blooms in Lake Taihu are highly dependent on wind direction and circulation, making it difficult to understand the process of nutrient release by field observations alone. Therefore, to fully understand the impact of cyanobacterial accumulation and decomposition on the nutrient profile of the aquatic environment, an experimental approach was taken to determine the potential influence of blooms on sediment nutrient release. Cyanobacterial and surface sediment layer samples were collected from Zhushan Bay in Lake Taihu during a cyanobacterial bloom event. Nutrient migration and transformation were assessed in water and sediments during decomposition of the cyanobacterial bloom. The primary objective of this study was to understand the potential influence of cyanobacterial bloom degradation on nutrient release from cyanobacteria across the whole lake environment. The changes in physical and chemical parameters were recorded in the waterbody during the experimental period, to help establish the influence of cyanobacterial bloom decomposition on sediment nutrient release. The results of this study further our understanding of the migration and transformation of nutrients during cyanobacterial accumulation and decomposition.

2 Materials and methods

2.1 Material preparation

The cyanobacteria and sediment samples assessed in this study were collected from Zhushan Bay, a typical cyanobacteria-dominated region located in the northwest of Lake Taihu (Fig. 1). Samples of cyanobacteria were collected using a phytoplankton capture network (PTN-S400, aperture 0.035 mm, Beijing Pu Lite Instrument Co., Ltd.), then rinsed three times with deionized water using a sieve to collect cyanobacteria (− 100 mesh~+ 200 mesh) in lab. Cyanobacteria were counted using a microscope (XSP-6C Shanghai Precision Instrument Co., Ltd.), with the cyanobacterial density altered to 5.0×10^{18} cells L^{-1} and then transferred to a 2000-mL capacity glass beaker. Cyanobacterial samples were then subjected to ultrasound (20 min, 25 °C, 2000 Hz) using an ultrasonicator (KQ-1000DE, Shanghai Precision Instrument Co., Ltd.). Finally, samples were sealed and frozen for use after being subjected to three consecutive freeze (− 20 °C) and thaw cycles, to ensure cyanobacterial cell lysis.

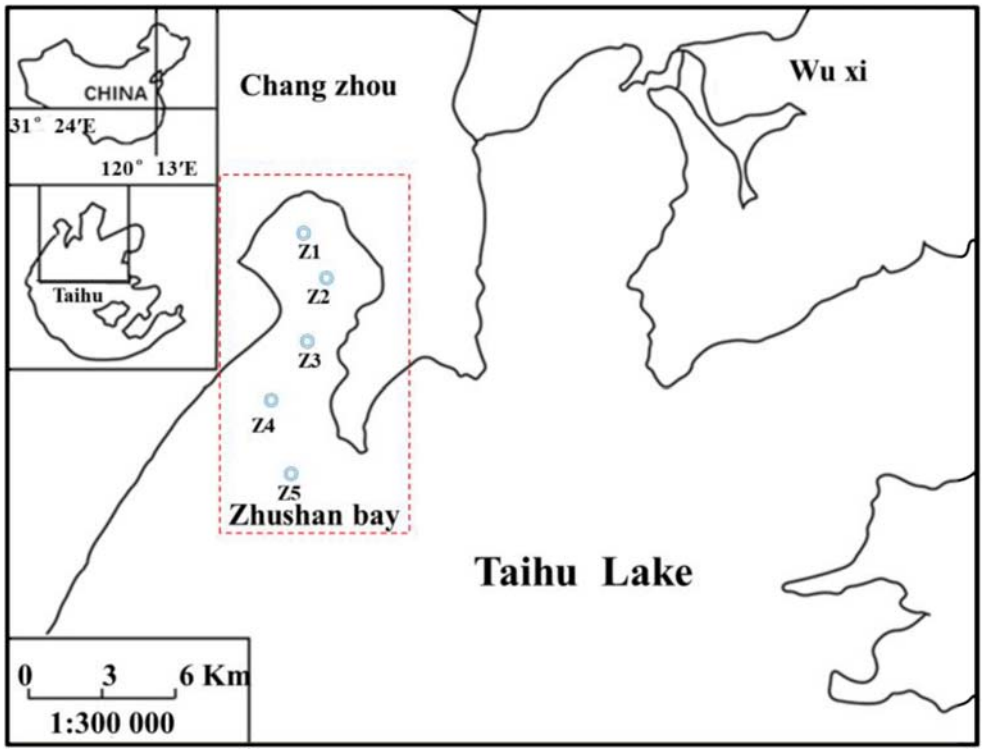

Fig. 1 Sampling site locations

Sediment samples were collected from the upper 15 cm of sediments using a sediment core sampler (Perrson MY-052, Mingyu Technology). Samples were returned to the laboratory and homogenized, dried in a freeze dryer (FD-1A-50, Beijing Bo Yikang Experimental Instrument Co., Ltd.), then ground and filtered through a 100-mesh sieve to remove benthic organism and large particulate matter, before being homogenized again, dried, and sealed for future use.

2.2 Experimental design

The experimental design comprised four parts (Table 1, Fig. 2). Each group was prepared in triplicate, and sealed with six layers of sterilized gauze in a plexiglass container (20-cm length × 20-cm width × 35-cm height), which was encased fully with opaque foil paper, then placed in a digital display light illumination incubator (MGC-400H Shanghai Yiheng Scientific Instrument Co., Ltd.). The experiment included assessment of the following: (1) physicochemical indicators and nutrient changes in water, including dissolved oxygen (DO), pH, electric conductivity (Ec), oxidation reduction potential (ORP), ultraviolet light (UV_{254}), total nitrogen (TN), nitrate nitrogen (NO_3^-–N), ammonia nitrogen (NH_4^+–N), TP, and soluble reactive phosphorus (SRP). (2) ΔC_w and ΔOM in the surface sediment. (3) The effects of cyanobacterial decomposition on the vertical distribution of nutrients in the sediment, including TN, NO_3^-–N, NH_4^+–N, TP, NaOH–P (Fe/AleP, P bound to Al, Fe and Mn oxides and hydroxides), BD-P (redox phosphorus), and HCl–P (CaeP, P associated with apatite). (4) The influence of cyanobacterial decomposition in N and P deposition, as well as the water-sediment flux.

2.3 Analytical methods

2.3.1 Analysis of water samples

Dissolved oxygen, pH, Ec, and ORP were measured using a multi-parameter water quality instrument (YSI6600, YSI (China) Limited); ultraviolet light (UV_{254}) was determined using a UV spectrophotometer (UV-5200, Shanghai Yuan Analysis Instrument Co., Ltd.); TN was determined via the alkaline potassium persulfate digestion method, followed by UV spectrophotometric analysis for NO_3^-–N detection using the cadmium reduction method, NH_4^+–N detection using Nessler's reagent photometry, TP detection by ammonium molybdate reagent photometry, and SRP detection using the molybdenum blue method after filtering through a 0.45-mm membrane (Shanghai Xingya Purifying Materials Factory, Q/IEE-1997) (Li et al. 2015; Cao et al. 2016)

The nutrients' release rate (υ) calculation formula for cyanobacterial decomposition is presented in Eq. (1):

$$\upsilon = \frac{\Delta C}{\Delta T} \tag{1}$$

where ΔC (mg L^{-1}) represents the difference in nutrient concentrations in water over a certain time interval; and ΔT (h) represents the time interval.

Table 1 The information of experimental design

Experiment	Group	Algae concentrations (cells/L)	Amount (algae-water mL or sediment cm^3)	Processing	Time (day)	Indexes	Fig.	Notes
Physicochemical parameters and nutrients change experiments in water	W_1–W_5	1.0×10^6, 1.0×10^8, 1.0×10^{10}, 1.0×10^{12}, 1.0×10^{15}	Plexiglass container Algae-water, 4000	Digital display light illumination incubator (35 °C 3000 lx)	0, 1, 5, 7, 9, 12, 15, 20, 25, 30	DO, pH, Ec, ORP, UV_{254}, TN, NH_4^+–N, NO_3^-–N, TP, SRP	Fig. 2a	
Surface sediment ΔC_w and ΔOM influence experiment	WS_0–WS_5	0, 1.0×10^6, 1.0×10^8, 1.0×10^{10}, 1.0×10^{12}, 1.0×10^{15}	Plexiglass container Algae-water, 4000 Sediment, 4000		0, 1, 5, 9, 20, 30.	C_w and OM	Figure 2B	▲
Investigation in the effects of cyanobacteria decomposition on the vertical distribution of nutrients in sediment	HS_0–HS_3	0, 1.0×10^8, 1.0×10^{12}, 1.0×10^{15}	Plexiglass container Algae-water, 4000 Sediment, 8000		0, 5, 10, 20, 30	TN, NH_4^+–N, NO_3^-–N,TP, NaOH–P, HCl–P, BD-P, NH_4Cl–P	Fig. 2c	●
Influence of N and P deposition during cyanobacteria decomposition and release flux in water-sediment	T_0–T_3	0, 1.0×10^8, 1.0×10^{12}, 1.0×10^{15}	Plexiglass container Algae-water, 4000 Sediment, 4000		0, 5, 10, 20, 30	TN, NH_4^+–N, NO_3^-–N, TP, SRP	Fig. 2d	★

▲ Based on the 0-day background value, the initial OM content was 1.56% ± 0.21%, and the average moisture content of the surface layer was 86.77% ± 5.32%, collected 0–5 cm deep to measured

● The initial background value were as follows (mg/g): TN (5.69), NH_4^+–N (1.06), NO_3^-–N (3.28), TP (0.65), NaOH–P (0.36), HCl–P (0.12), BD-P (0.05), NH_4Cl–P (0.03)

★ Supernatant was taken as the pore water after placing 10 mL of surface sediment (0–5 cm) into a test tube and centrifuging at 5000 rpm for 10 min

2.3.2 Analysis of sediment samples

An aliquot of fresh sediment material was transferred to a Petri dish and weighed, then placed in an oven at 110 °C for 12 h (HB841-0, Suzhou Hao Bei Energy Saving Oven Factory). Next, the dried samples were weighed on an aseptic console after 1 h allowing the moisture content of surface sediments to be calculated according to Eq. (2) (Zhang et al. 2017). Briefly, 2 g of dried sediment was placed in a crucible, sealed and heated in a muffle furnace (FD-40, Shanghai Hegong Scientific Instrument Co., Ltd.) at 550 °C for 2 h. Loss on ignition (LOI) was used to reflect the organic content of the sediment material (Murphy et al. 2010; Tisdall and Oades 2010).

$$C_w = \frac{W_0 - W_{110}}{W_0} \times 100\% \quad (2)$$

$$\mathrm{OM\ (LOI)} = \frac{W_{110} - W_{550}}{W_{105}} \times 100\% \quad (3)$$

where C_w represents the moisture content of sediments; W_0 is the weight of the fresh sediment sample material; W_{110} is the weight of the sediment sample material after drying at 110 °C; and W_{550} is the weight of the sediment after heating to 550 °C.

Sediment samples were pretreated by freeze-drying for 24 h, ground and then passing through a 100-mesh sieve, before being treated according to the standard measurements and testing (SMT) method (Ruban et al. 2001) and the alkaline extraction method (Brodrick et al. 1987).

2.3.3 Analysis of cyanobacterial samples

The cyanobacterial density was determined microscopically (XSP-6C Shanghai Precision Instrument Co., Ltd.) and the corresponding dry weight was established. The sample densities (d.w.) applied for experiments were 1.0×10^6 cells L^{-1} (25.3 ± 5.32 mg L^{-1}), 1.0×10^8 cells L^{-1} (112.5 ± 11.25 mg L^{-1}), 1.0×10^{10} cells L^{-1} (226.7 ± 9.91 mg L^{-1}), 1.0×10^{12} cells L^{-1} (825.5 ± 23.96 mg L^{-1}), and 1.0×10^{15} cells L^{-1} (2068.2 ± 35.77 mg L^{-1}).

2.3.4 Relationship between cyanobacterial density, nutrient concentrations in water, sediment organic matter, and moisture content

The relationship between dry weight of the cyanobacterial pulp and the maximum nutrient content of each experimental group (W_1–W_5), the maximum increase in organic matter ($\Delta OMmax_i$), and the increase in moisture content ($\Delta C_w max_i$) from WS_1 to WS_5 were determined according to Eq. (4) and Eq. (5):

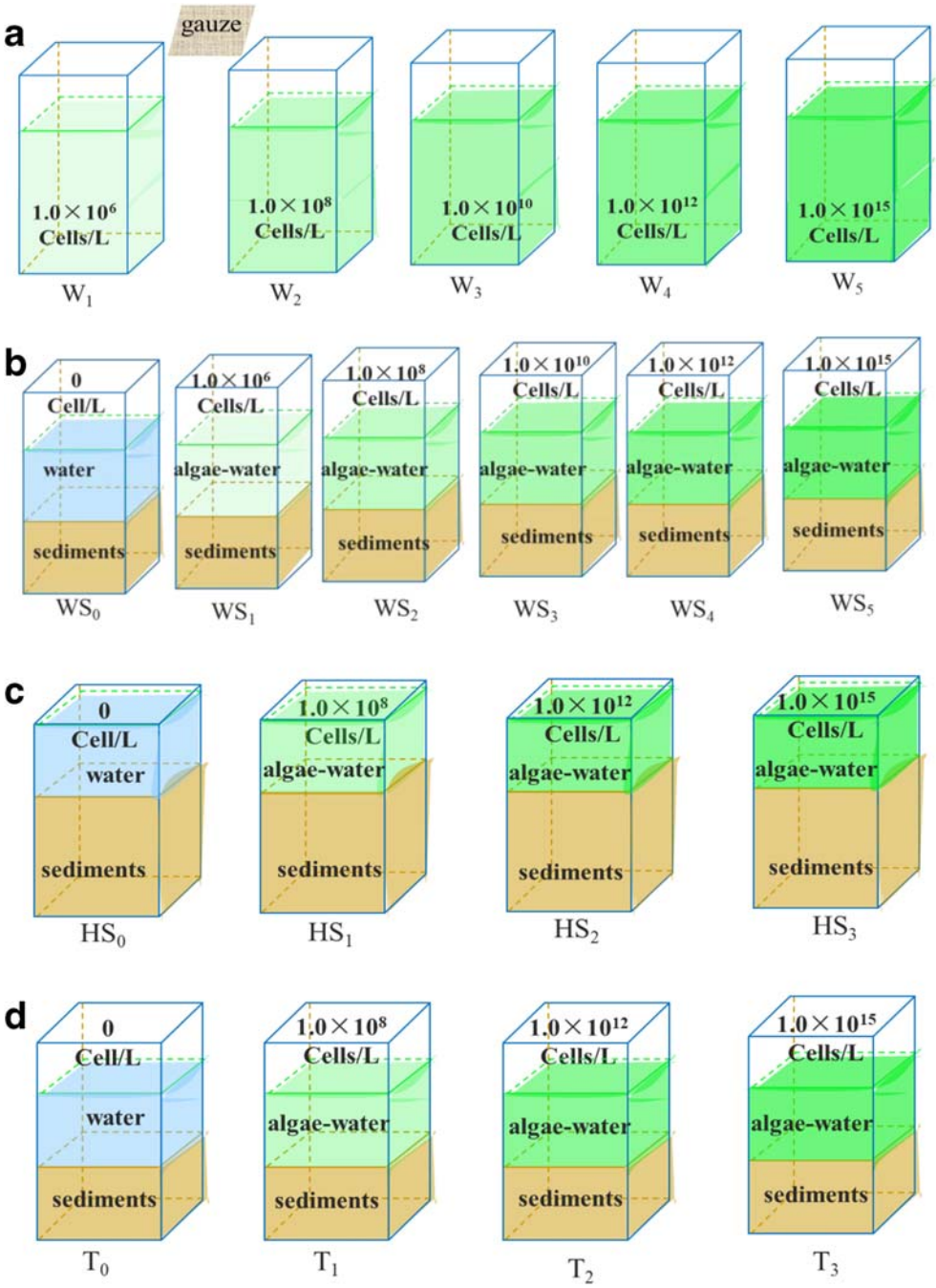

Fig. 2 **a**–**d** Schematic diagram of experimental design

$$\Delta\mathrm{OMmax}_i = \mathrm{OMmax}_i - \mathrm{OM}ws_0 \quad (4)$$

where OMmax_i is the maximum amount of organic matter in the experimental group (i) and $\mathrm{OM}ws_0$ is the average amount of organic matter in the control group.

$$\Delta\mathrm{C}_W\mathrm{max}_i = C_w\mathrm{max}_i - C_W ws_0 \quad (5)$$

where $C_w\mathrm{max}_i$ is the maximum moisture content value in the experimental group (i), and $C_W ws_0$ is the average moisture content value in the control group.

2.3.5 Analysis of water-sediment nutrient flux

The nutrients' concentration gradient method was used to determine the deposition and release of nutrients during cyanobacterial decomposition (Herrera-Silveira et al. 2002) as described in Eq. (6):

$$F = f_\mathrm{d} + f_\mathrm{a} + f_\mathrm{s} \quad (6)$$

where F is the net flux at the water-sediment interface; f_d is the molecular diffusion flux due to differences in nutrients'

concentration at the interface; f_a is the amount of advection of pore water in sediments, and f_s is the diffusion flux produced by solid particle deposition.

$f_a + f_s$ is negligible relative to the molecular diffusion flux and, therefore, Eq. (6) can be simplified to Eq. (7):

$$F \approx f_d \tag{7}$$

where f_d was calculated by Fick's first law (Lavery et al. 2010; Zastepa et al. 2017), as defined by Eq. (8):

$$f_d = \Phi \times D_s \times \frac{\delta_c}{\delta_x} \tag{8}$$

where f_d is the nutrient diffusion flux at the sediment-water interface (μmol m^{-2} day^{-1}); Φ is the average porosity of the upper surface of the sediment (1–5 cm) (reported for Lake Taihu as 0.60) (Bai and Zhou 2012; Cheng et al. 2015); D_s is the diffusion coefficient for the sediment block and $D_0$is the diffusion coefficient for the ideal solution ($\Phi < 0.7$, $D_s = \Phi D_0$; $\Phi \geq 0.7$, $D_s = 2\Phi D_0$) (Ram et al. 2009). For P and N, D_0 were applied as 19.8×10^{-6} cm s^{-1} and 7.34×10^{-6} cm s^{-1}, respectively (Forster et al. 1999; Grasso et al. 2011); $\frac{\delta_c}{\delta_x}$ represents the difference between the nutrient concentrations in the pore water and overlying water (with $\frac{\delta_c}{\delta_x} < 0$ and $f_d < 0$ indicating sediment deposition; otherwise, sediment release is indicated) (Iversen and Bo 1993; Wieland et al. 2003).

2.4 Data handling and statistical analysis

Data are expressed as the mean value ± standard deviation (SD). Analysis for significance was conducted using SPSS software (SPSS 22.0, USA), with $p < 0.05$ considered to be significant. Equation fitting was performed using Origin (Origin 8.6, USA, OrigiLa) and R (R3.5.2, The University of Auckland, Ross Ihaka and Robert Gentleman) software.

3 Results and discussion

3.1 Physicochemical indices and change in nutrient concentrations in water

3.1.1 Trends in pH, DO, Ec, ORP, and UV_{254} in water

Generally, pH initially decreased from 0 to 10 days and then increased from 10 to 30 days (Fig. 3a), although significant differences were visible between experimental groups ($p < 0.05$). The decrease in pH occurred due to algal cell decomposition and the release of large amounts of CO_2 and organic acids into water (Maagd et al. 1999). Group W_5 showed the greatest change, with a pH of only 3.88 on day 9. However, as organic matter is consumed by microorganisms, the pH value of water gradually increased, eventually becoming alkaline (Chen et al. 2018a, b, c). This is shown by the results of the present study, where pH gradually increased until reaching 8.26 (W_5) at the end of the experimental period. DO is an important indicator of water quality (Kaiho 1994; Atkinson et al. 2007) and in experimental groups, the DO concentration generally decreased rapidly (Fig. 3b). The reduction in DO occurs as degradation of organic matter consumes DO in water (Shi et al. 2017), while cyanobacterial debris forms a membrane on the water surface, hindering the dissolution of oxygen from the air (Trimmer et al. 2003). After 24 h, with the exception of group W_1, the DO concentration was less than 2.0 mg L^{-1} in all experimental groups, with W_5 containing only 0.15 mg L^{-1} DO, while W_1 was significantly different to the other four groups ($p < 0.05$).

Oxidation reduction potential reflects the macroscopic oxidation reduction properties exhibited cumulatively by all substances present in the system and is used to characterize the relative strength of the oxidative or reductive properties of the medium (Masscheleyn et al. 1990). As shown in Fig. 3 c, during cyanobacterial decomposition, the ORP value decreased significantly within 24 h and the water status changed from an oxidized to a reduced state. In the W_1 group, ORP showed significant differences ($p < 0.05$) among all experimental groups. At the end of the experimental period, ORP in groups W_1–W_5 were − 86.11 mv, − 161.88 mv, − 247.38 mv, − 378.22 mv, and − 427.03 mv, respectively, which is in accordance with the findings of previous studies (Xie et al. 2004; Wu et al. 2017). Ec increased in all experimental groups and tended to become stable after 12 days, with group W_5 reaching a maximum of 792.5 μs cm^{-1} (Fig. 3d). The Ec was significantly different across all experimental groups ($p < 0.05$). The increase in Ec indicates that the decomposition of cyanobacteria leads to a larger concentration of total dissolved solids (TDS, mg L^{-1}) and, therefore, enhances conductivity (Chuai et al. 2011; Mukherjee et al. 2014).

The UV_{254} is commonly used as a comprehensive indicator for determining the level of integrated organic matter contamination in water bodies, as most organic matter in water exhibits absorption peaks at 254 nm (Russo et al. 2018). For example, the UV_{254} is well correlated with various water quality indicators, such as COD. Some previous studies have used $SUVA_{254}$ to determine the organic matter content or humus level of organic matter, indicating the ratio of the absorption coefficient at 254 nm to the DOC concentration of water (Russo et al. 2018; Ye et al. 2018). Larger $SUVA_{254}$ values indicate a greater molecular weight, humification level, and aromaticity of organic matter in water (Yang et al. 2014). As shown in Fig. 3 e, in all experimental groups, the UV_{254} tended to decrease after an initial increase, indicating that organic matter gradually increased during cyanobacterial decomposition and that

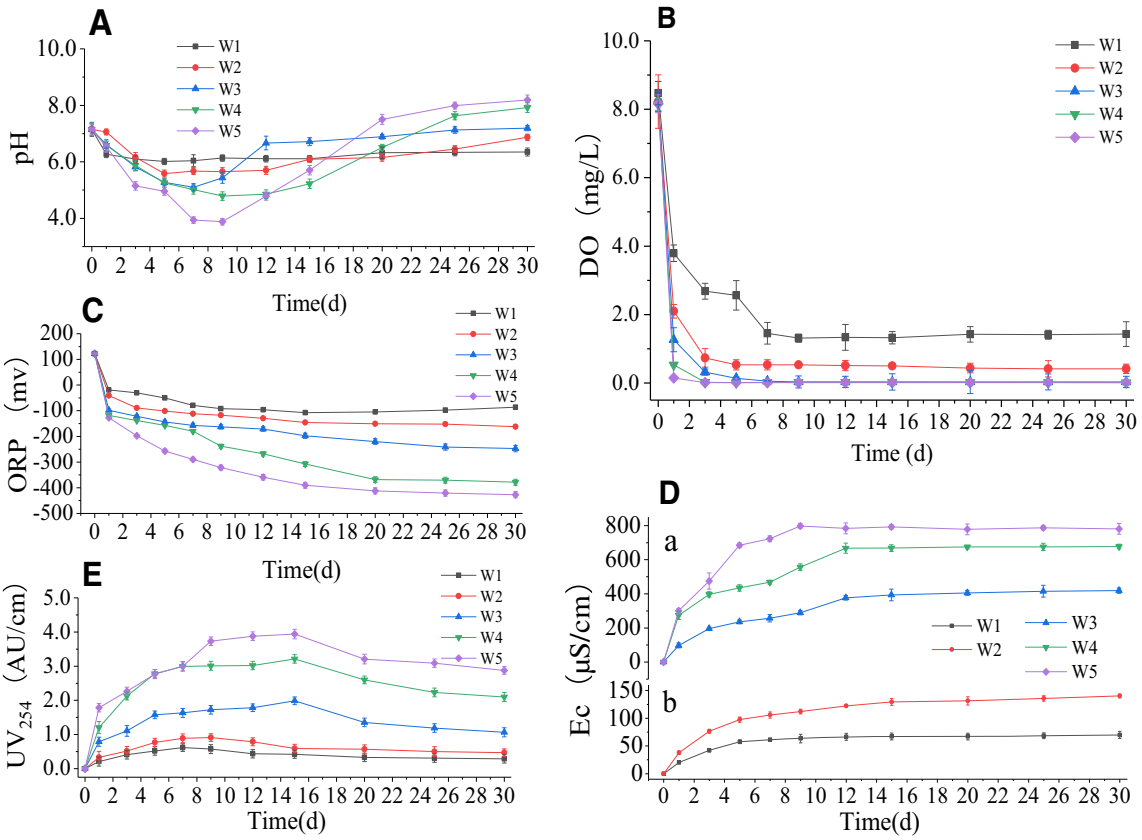

Fig. 3 **a**–**e** pH, DO, Eh, Ec, and UV_{254} change in water during cyanobacteria decomposition

macromolecular organic matter was decomposed into small molecular organic matter after 15 days.

3.1.2 Trends in TN, NH_4^+–N, NO_3^-–N, TP, and SRP concentrations in water

During the initial experimental period, cyanobacteria began to decay and release nutrients, causing the TN concentration to increase (Fig. 4a). However, due to species differences in cyanobacterial density, varying trends in N-form were observed. The TN concentration in the W_1 and W_3 groups reached a maximum of 6.99 mg L^{-1} and 67.88 mg L^{-1} at 9 days, respectively. On day 12, the highest concentrations in groups W_2 and W_4 were 20.22 mg L^{-1} and 122.79 mg L^{-1}, respectively, while W_5 reached a maximum of 232.55 mg L^{-1} on day 15. The increase in TN in groups W_1–W_5 were 0.78 mg L^{-1} day^{-1}, 7.55 mg L^{-1} day^{-1}, 1.69 mg L^{-1} day^{-1}, 10.79 mg L^{-1} day^{-1}, and 15.5 mg L^{-1} day^{-1}, respectively. In the subsequent decomposition process, microorganisms and the anaerobic environment caused N species in the water to gradually be converted to stable NH_4^+–N, which resulted in a gradual increase in NH_4^+–N during the initial stages of the experimental process (Fig. 4b). The water also initially contained a high DO content (Li et al. 2015; Cao et al. 2016; Dai et al. 2018). Granules and macromolecular organic nitrogen from decomposed cyanobacteria were initially oxidized to NO_3^-–N (Cao et al. 2016; Dai et al. 2018) and as oxygen was consumed, part of the NO_3^-–N was converted to NH_4^+–N (Li et al. 2015). Therefore, the initial increase in NO_3^-–N was then followed by a decrease (Fig. 4c). After day 15, N in each form decreased to different degrees. Denitrification was enhanced in the anaerobic reductive environment, with N released into the atmosphere in the form of N_2 or N_2O (Kuanyi et al. 2010), which is one of the main pathways causing an overall decrease in N content.

The TP concentrations in the water of each experimental group gradually increased (Fig. 4d). The highest concentrations in groups W_1–W_5 were 0.67 mg L^{-1} on day 9, 1.21 mg L^{-1} on day 20, 2.21 mg L^{-1} on day 35, 5.18 mg L^{-1} on day 15, and 7.63 mg L^{-1} on day 12. The increase in TP in groups W_1–W_5 was 0.074 mg L^{-1} day^{-1}, 0.061 mg L^{-1} day^{-1}, 0.073 mg L^{-1} day^{-1}, 0.345 mg L^{-1} day^{-1}, and 0.636 mg L^{-1} day^{-1}, respectively. The SRP increased with degradation time (Fig. 4e), with the proportion of SRP in TP increasing gradually throughout the experimental period. In the early stages of degradation, high concentrations of dissolved organic phosphorus were present in the water, with organic phosphorus

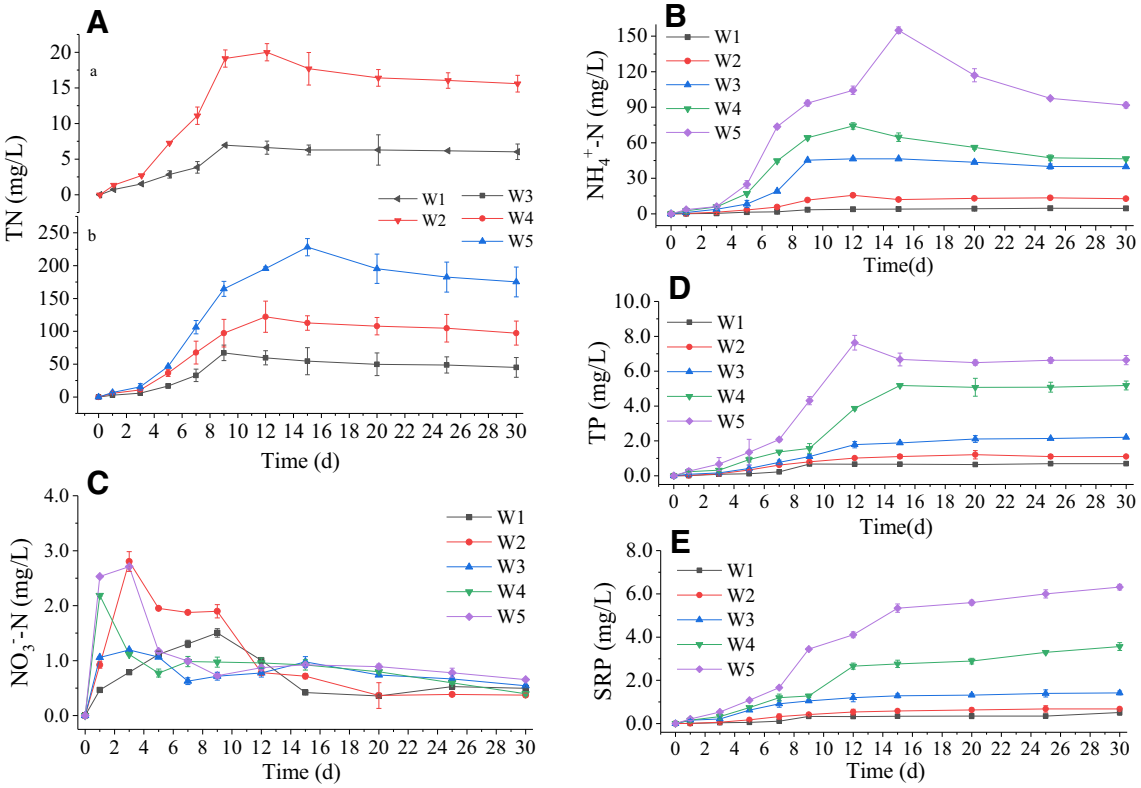

Fig. 4 **a**–**e** Changes in water TN, NH_4^+–N, NO_3^-–N, TP, and SRP during cyanobacteria decomposition

mineralized into inorganic phosphorus by microorganisms (Yu et al. 2018), therefore increasing the SRP content. At the end of the experimental period, the relative proportions of SRP in TP in groups W_1–W_5 were 49.33%, 52.56%, 67.34%, 68.77%, and 81.12%, respectively. These results show that nutrients undergo transitions between various forms during cyanobacterial decomposition.

3.2 Variations in ΔOM and ΔC_w in the surface sediment layer

The OM is an active substance in surface sediments that can be adsorbed, distributed, and complexed with other pollutants such as heavy metals and organic matter. The content and distribution of OM can be used to evaluate organic nutrients levels in surface sediments (Akagi and Zsolnay 2008; Mccabe and Arnold 2017; Haas et al. 2018). The degradation of organic matter in surface sediments consumes a large amount of DO, forming an anaerobic environment. Simultaneously, research has shown that high levels of nutrient release increase the risk of deterioration of water quality (Keil et al. 1994; Fujii et al. 2018).The OM content of the surface sediment layer of each experimental group increased in the pre-cyanobacterial decomposition period (Fig. 5a), which was significantly different from that of WS_0 ($p < 0.05$). The peak OM contents in experimental groups W_1–W_5 were 2.09% on day 9, 3.70% on day 9, 5.16% on day 5, 7.57% on day 5, and 9.21% on day 5, respectively.

As shown in Fig. 5 a, during the first 9 days of the experimental period, the OM concentrations in the surface sediment increased in accordance with both time and cyanobacterial concentration. This pattern is likely to have occurred because most cyanobacteria existed in colonies when they were added to the experimental environment. During the decomposition process, the colloidal coating surrounding cyanobacterial groups was degraded, allowing colonies to be broken up and resulting in decreased buoyancy and an increase in sedimentation. Moreover, the sedimentation velocity of cyanobacterial debris was greater than the degradation rate, with cyanobacterial particles found on the surface of the sediment during the experimental period, which is an important factor leading to the rapid increase in organic matter content in the surface sediment. In addition, studies have shown that cyanobacterial accumulation accelerates the sedimentation of suspended solids in water, thereby accelerating the increase in organic matter

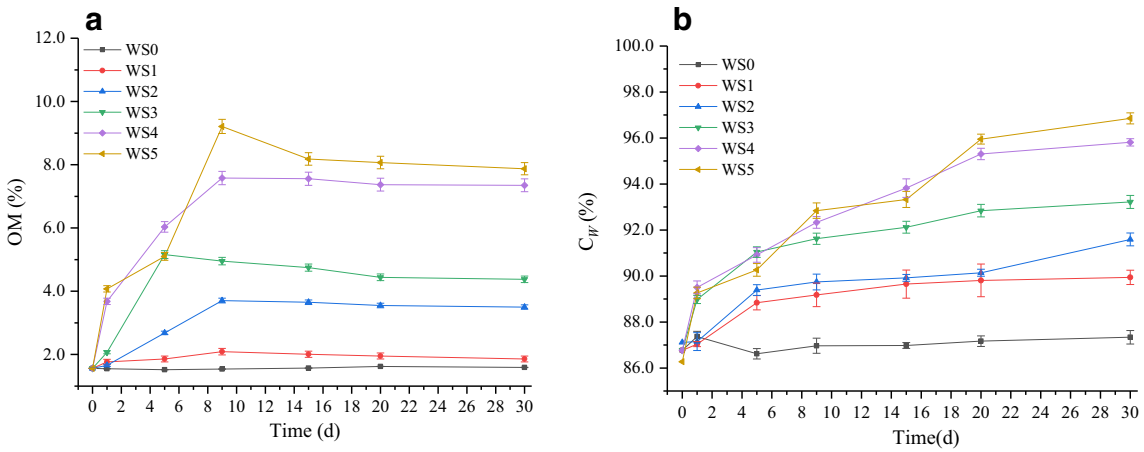

Fig. 5 **a**, **b** Change in OM and C_w in surface sediment during cyanobacteria decomposition

content in surface sediments (Queiroz et al. 2007; Henderson et al. 2008; Wert and Rosarioortiz 2013). Moreover, organic microbial residues in the water and microbial products such as intermediate decomposition products and metabolites may also cause an increase in OM (Cory and Kling 2018).

The sediment moisture content reflects the porosity of the sediment and is inversely proportional to sediment particle size, which affects the resuspension of sediments (Aigars 2001). The sediment resuspension process is an important way for nutrients and OM in sediments to be exchanged and redistributed between sediments and overlying water (Seelen et al. 2018).Therefore, surface sediment layer moisture content is an important parameter for assessing water-sediment nutrient exchange (Matisoff et al. 2017). The effects of cyanobacterial decomposition on the moisture content of surface sediments are shown in Fig. 5 b. Overall, cyanobacterial decomposition led to an increase in sediment surface layer moisture levels, reaching 89.94%, 91.59%, 93.22%, 95.81%, and 96.85% in groups W_1–W_5, respectively, compared to 87.33% in W_0 (control group). Significant differences were observed between the experimental groups and the control group in all cases ($p < 0.05$).

As shown in Fig. 5 a and b, during the first 9 days of the experimental period, the accumulation of large OM promoted an increase in moisture content in the surface sediment layer, further accelerating the sedimentation of suspended solids and resulting in increased moisture content in the surface sediment layer. Moreover, the deposited cyanobacterial debris provides a good breeding environment for microorganisms (Henderson et al. 2008), increasing the microbial content of sediments (Queiroz et al. 2007). Microbial accumulation affects the porosity of the surface sediment layer (Wert and Rosarioortiz 2013) and therefore changes the surface sediment layer moisture content. Moreover, during large-scale cyanobacterial reproduction, aggregation, and decomposition, the interaction between cyanobacteria and microbes in the sediment would contribute to the formation of gas products (e.g., CH_4, H_2S and CO_2…), causing bubbles to appear on the surface of the sediment, further changing the sediment moisture levels (Lei et al. 2014; Sörensson Shiraishi et al. 2017).

3.3 Relationship between cyanobacterial accumulation and nutrient content in water and between $\Delta OMmax_i$ and $\Delta C_w max_i$ in surface sediments

The relationship between the maximum release of nutrients in water (TN, NH_4^+–N, NO_3^-–N, TP, SRP) and cyanobacterial density is shown in Fig. 6 a–e, with data fitting performed using Eqs. (9)–(13) as follows:

$$Y_{\mathrm{TN(mg/L)}} = 9.56922 + 0.16984 \times X - 3.1185\mathrm{E}{-5} \times X^2 \quad (R^2 = 0.98196) \tag{9}$$

$$Y_{\mathrm{NH4+-N(mg/L)}} = 9.50186 + 0.09461 \times X - 1.1876\mathrm{E}{-5} \times X^2 \quad (R^2 = 0.97507) \tag{10}$$

$$Y_{\mathrm{NO3^-\text{-}N(mg/L)}} = 2.024525 - 0.0021 \times X + 3.78088\mathrm{E}{-5} \times X^2 - 1.25828\mathrm{E}{-9} \times X^3 \quad (R^2 = 0.29473) \tag{11}$$

$$Y_{\mathrm{TP(mg/L)}} = 0.52718 + 0.00717 \times X - 1.80816\mathrm{E}{-5} \times X^2 \quad (R^2 = 0.99902) \tag{12}$$

$$Y_{\mathrm{SRP(mg/L)}} = 0.32614 + 0.00462 \times X - 8.3221\mathrm{E}{-7} \times X^2 \quad (R^2 = 0.99694) \tag{13}$$

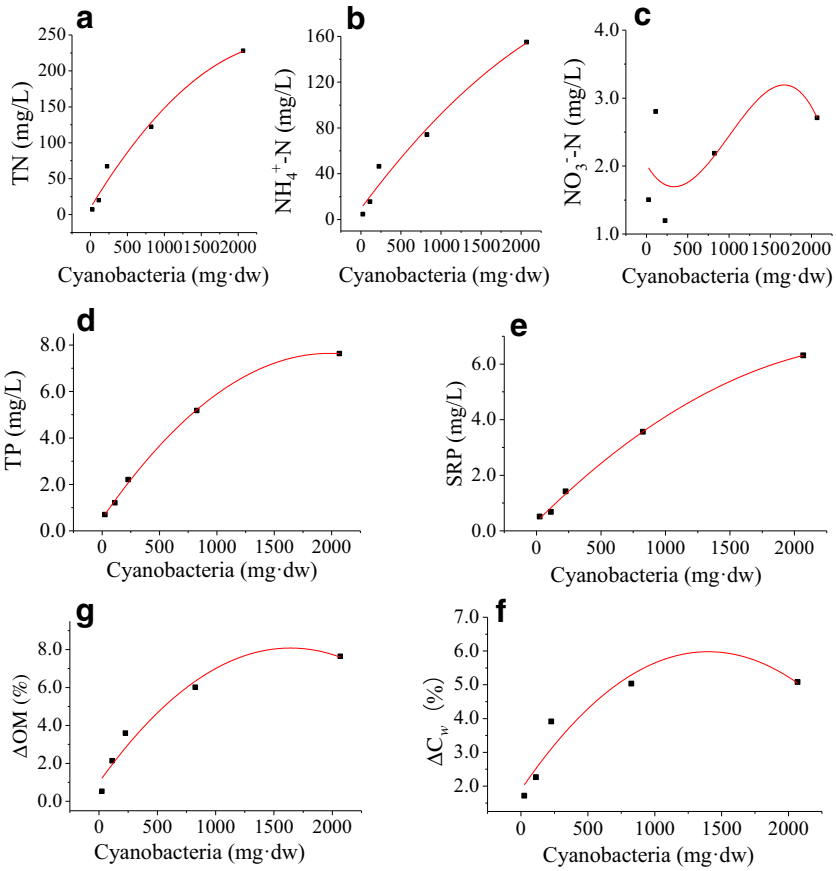

Fig. 6 **a**–**g** Relationship between cyanobacteria decomposition and nutrients in water, $\Delta OMmax_i$ and $\Delta C_w max_i$ in surface sediment

Results show that all data exhibited a good binomial curve fit ($R^2 > 0.90$, $p < 0.05$), with the exception of NO_3^-–N ($R^2 = 0.29473$, $p > 0.05$), which may be due to the instability of NO_3^-–N (Gkelis et al. 2014).

The fitting relationship associates the $\Delta OMmax_i$ and $\Delta C_w max_i$ in surface sediments with cyanobacterial weight during decomposition, as shown in Fig. 6 f and g. This relationship can be described according to Eqs. (14) and (15) as follows:

$$Y\Delta C_w max_i(\%) = 1.89182 + 0.00585 \times X - 2.08578E-6 \times X^2 \quad (R^2 = 0.90887) \quad (14)$$

$$Y\Delta OMmax_i(\%) = 0.9992 + 0.00871 \times X - 2.6321E-6 \times X^2 \quad (R^2 = 0.96299) \quad (15)$$

Results show that data exhibit a good binomial relationship ($R^2 > 0.90$, $p < 0.05$), indicating that cyanobacteria have an effect on the moisture content and organic matter content of surface sediments during cyanobacterial sedimentation and decomposition.

3.4 Vertical distribution of nutrients in sediments

As shown in Fig. 7 a, TN is upregulated over time in the D_1 and D_2 layers, as cyanobacterial density increased. The TN content reached a maximum value of 157.85 mg g^{-1} in the D_1 layer on day 20 in the HS_3 group. D_3 and D_4 only showed slight increases in the later stages of the experimental period, increasing by 1.32 mg g^{-1} and 5.66 mg g^{-1}, respectively. NH_4^+–N (Fig. 7b) concentrations in the D_1 layer increased significantly with increased cyanobacterial density, reaching 121.42 mg g^{-1} in the HS_3 group on day 15, while in groups D_1, D_2, and D_3, they reached maximum values of 4.56 mg g^{-1}, 3.23 mg g^{-1}, and 9.89 mg g^{-1}, respectively, on day 20 in the HS_2. The degradation of high-density cyanobacterial blooms causes surface sediments to rapidly enter an anaerobic state (Keil et al. 1994; Christine Laskov et al. 2002; Fujii et al. 2018), which accelerates the increase in NH_4^+–N. NO_3^-–N (Fig. 7c) concentrations initially increased, then decreased in D_1 and D_2 layers. A significant increase in NO_3^-–N occurred in accordance with algal density, until maximum values of 5.89 mg g^{-1} and 3.87 mg g^{-1} were achieved in the HS_3 group D_1 and D_2 layers on day 15, respectively. Conversely, in the D_3 and D_4 layers, the NO_3^-–N concentration gradually reduced.

The TP concentrations (Fig. 7d) gradually increased with time, showing sediment surface deposition. TP concentrations reached a maximum of 3.76 mg g^{-1} on day 20 in the HS_2 group, with the increase in TP content occurring due to an accumulation of algal or biological residues in the upper sediment. NaOH–P concentrations (Fig. 7e) gradually increased

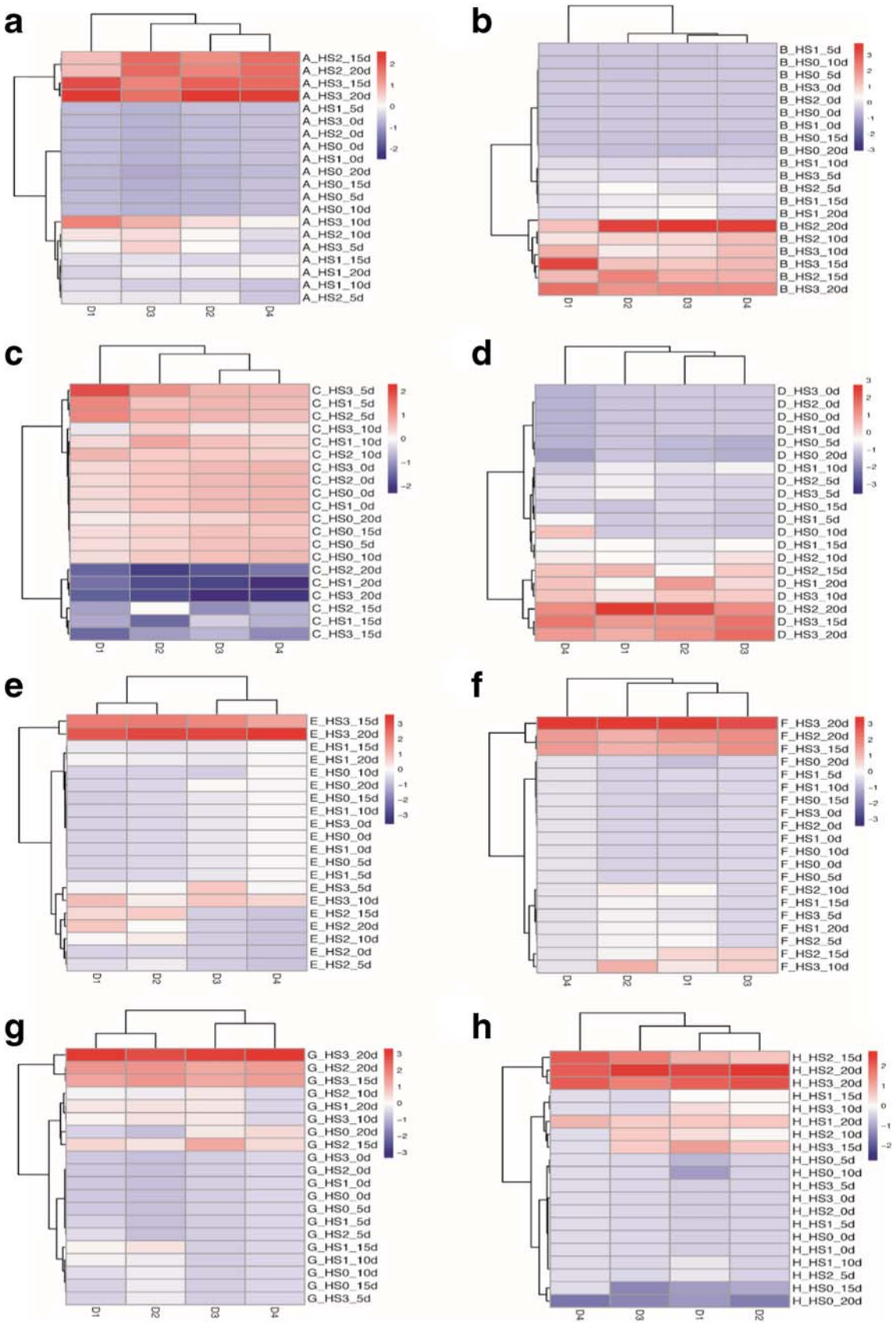

Fig. 7 N and P vertical distribution in bottom mud. D_1, 0–5 cm; D_2, 5–10 cm; D_3, 10–15 cm; and D_4, 15–20 cm. A_HSi_0 d, where **a** is TN, **b** is NH_4^+–N, **c** is NO_3^-–N, **d** is TP, **e** is NaOH–P, **f** is HCl–P, **g** is BD-P, **h** is NH_4Cl–P, HSi is a representative experimental group, and *d* is the number of days of degradation

Table 2 Flux of different forms of nitrogen and phosphorus nutrients ($mg \cdot m^{-2} \cdot day^{-1}$)

Group	Time (day)	TN	NH_4^+–N	NO_3^-–N	TP
T_0 (control)	1	26.61 ± 4.75	3.08 ± 0.97	9.37 ± 1.33	3.62 ± 1.01
	5	16.99 ± 2.31	1.93 ± 0.05	3.89 ± 0.98	2.33 ± 0.92
	10	13.16 ± 2.11	1.60 ± 0.13	2.17 ± 0.96	1.72 ± 0.72
	20	10.76 ± 1.22	1.27 ± 0.77	1.75 ± 0.92	1.29 ± 0.09
	30	9.63 ± 1.02	0.99 ± 0.06	1.59 ± 0.07	0.77 ± 0.02
	Average	15.43 ± 1.03	1.77 ± 0.08	3.75 ± 0.11	1.95 ± 0.07
T_1 (low)	1	2.43 ± 0.79	11.49 ± 1.23	6.60 ± 0.51	1.72 ± 0.02
	5	− 1.9 ± 0.06	4.43 ± 0.96	4.81 ± 1.01	1.02 ± 0.05
	10	− 7.97 ± 0.97	− 8.86 ± 0.72	2.13 ± 0.03	− 0.85 ± 0.05
	20	− 10.22 ± 1.03	− 7.28 ± 0.98	4.00 ± 1.01	− 0.93 ± 0.03
	30	− 11.11 ± 1.15	− 6.26 ± 1.11	1.67 ± 0.59	− 0.66 ± 0.04
	Average	− 5.75 ± 0.23	− 1.29 ± 0.06	3.84 ± 0.11	0.06 ± 0.02
T_2 (medium)	1	4.98 ± 0.88	− 0.41 ± 0.02	5.82 ± 1.17	1.54 ± 0.22
	5	− 38.91 ± 8.23	− 20.78 ± 3.77	5.29 ± 1.01	0.23 ± 0.02
	10	− 163.68 ± 6.99	− 132.65 ± 12.11	5.09 ± 0.91	− 1.90 ± 0.03
	20	− 98.38 ± 7.31	− 110.55 ± 9.22	4.41 ± 1.25	− 2.67 ± 0.07
	30	− 57.53 ± 4.66	− 75.75 ± 5.31	3.44 ± 0.98	− 1.34 ± 0.09
	Average	− 70.70 ± 6.57	− 68.03 ± 5.32	4.81 ± 1.02	− 0.83 ± 0.11
T_3 (high)	1	− 6.83 ± 1.56	− 5.23 ± 1.11	− 6.07 ± 2.13	1.04 ± 0.07
	5	− 119.64 ± 9.33	− 29.04 ± 3.22	− 1.66 ± 0.56	− 1.98 ± 0.07
	10	− 224.78 ± 11.88	− 123.17 ± 13.33	4.93 ± 0.99	− 9.26 ± 1.22
	20	− 259.81 ± 17.11	− 147.87 ± 8.66	0.69 ± 0.05	− 13.28 ± 1.01
	30	− 99.67 ± 5.77	− 34.42 ± 3.22	1.04 ± 0.33	− 11.21 ± 1.77
	Average	− 142.15 ± 10.31	− 67.95 ± 7.22	− 0.214 ± 0.02	− 6.94 ± 1.05

in the D_1 and D_2 layers, reaching a maximum of 1.83 mg g^{-1} on day 20 in the HS_3 group. Cyanobacterial decomposition induces an anaerobic environment at the sediment surface, in which Fe^{3+} is reduced to Fe^{2+} and NaOH–P is released into the water with the dissolution of Fe^{2+} (Christophoridis and Fytianos 2006). Simultaneously, P is adsorbed onto Fe, Al, and hydroxides and is also released into the interstitial water, migrating to the surface sediment layer (Chen et al. 2018a, b, c), resulting in enrichment of the NaOH–P content in the D_1 layer. HCl–P concentrations reached a maximum value of 0.51 mg g^{-1} on day 20, in the D_1 layer in the HS_3 group (Fig. 7f). This occurred because during the later stage of cyanobacterial degradation, the pH of water was between 7 and 9, with increased pH conditions being beneficial to the conversion of various forms of P to HCl–P (Jiao et al. 2016). A previous study by Jin et al. (2006) supported these findings, suggesting that pH controlled the concentrations of available Fe, Al, and calcium, directly or indirectly altering both biological and chemical reactions (Jin et al. 2006). The rate of P release decreased as the pH increased from 2 to 6, then increased as the pH increased further from 8 to 12 (Jin et al. 2006). The BD-P concentration (Fig. 7g) increased with the decomposition of cyanobacteria in the sediment, due to the consumption of DO in the waterbody and enhanced anaerobic microbial activity, promoting the release of BD-P (Kleeberg and Kozerski 1997). Overall, the degree of change in BD-P concentration at different sediment depths was ranked in the descending order of $D_1 > D_2 > D_3 > D_4$. NH_4Cl–P (Fig. 7h) is unstable and readily adsorbed (Jin et al. 2006), with suspended particles produced by cyanobacterial decomposition adsorbing NH_4Cl–P and depositing it on the surface sediment layer during sedimentation. The concentration of NH_4Cl–P reached a maximum value of 0.13 mg g^{-1} on day 20 in the HS_2 group D_1 layer. This was due to the instability of NH_4Cl–P and the occurrence of migration between sediment layers over time (Stone and English 1993), resulting in slow changes in the underlying sediment nutrient profiles. These results are partially consistent with the reported findings of a previous study on sediment nutrient profiles in a eutrophic region of Lake Taihu (Jin et al. 2006).

3.5 Effect of cyanobacterial decomposition on the water-sediment nutrient flux

Flux results are shown in Table 2, with various nutrients in the control (T_0) group showing an overall water trend of being released into the water ($f_d > 0$). TN began to show sedimentation from day 5 ($f_d < 0$) in group T_1. After day 10, with the

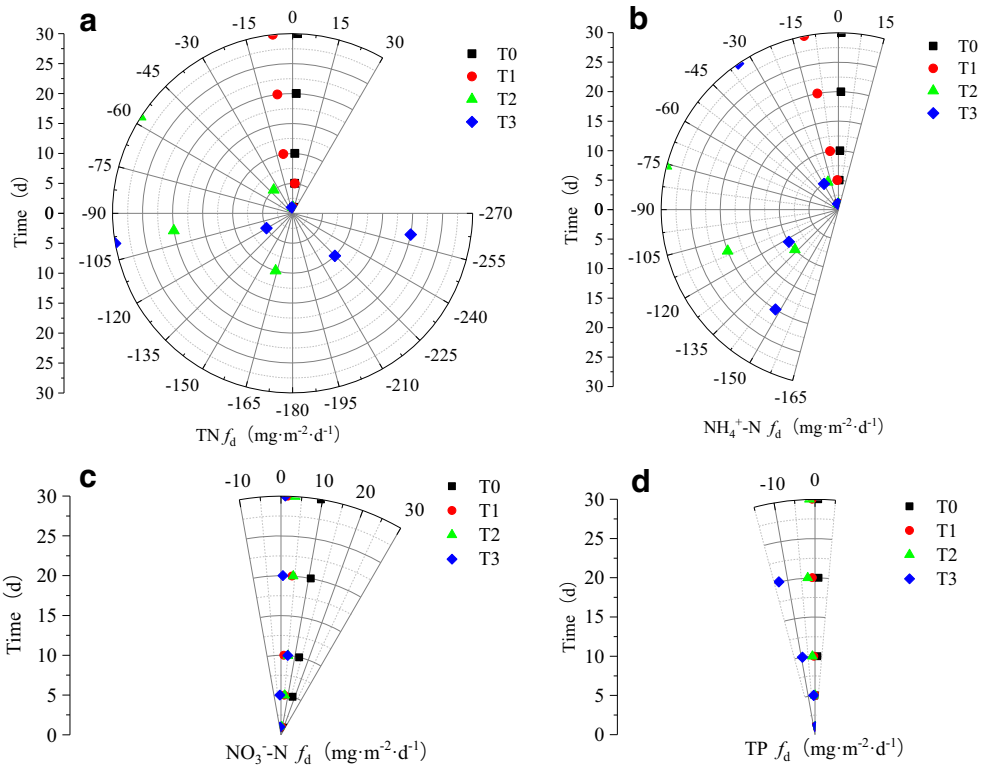

Fig. 8 Polar diagram (r, θ) of different nutrient fluxes

exception of nitrate nitrogen ($f_d > 0$), all other nutrients showed a sedimentation response ($f_d < 0$), with group T_2 presenting a similar pattern to T_1. In the T3 group, with the exception of TP which showed deposition after five days, all other nutrients entered the sedimentation mode within 24 h. The deposition of nutrients increased as the density of cyanobacteria increased, as shown by the polar diagram (r, θ) of nutrient flux (Fig. 8), with flux amplitude ranked in the descending order of TN > NH_4^+–N > NO_3^-N > TP. TN was mainly deposited during the process of cyanobacterial accumulation and decomposition (Fig. 8a), with the highest flux observed in group T_3 on day 20 (− 259.81 mg m^{-2} day^{-1}) and a significant difference between the control group and the experimental group ($p < 0.05$). The change in NH_4^+–N flux was similar to the pattern observed for TN (Fig. 8b). However, the overall variation and flux intensity were weaker for NH_4^+–N than TN, with the highest NH_4^+–N flux observed on day 20 in group T_3 (− 147.87 mg m^{-2} day^{-1}). Due to the instability of NO_3^-–N, it was released in other groups (T_1 and T_2), with the exception of alternating release and deposition with time in group T_3 (Fig. 8c). Although TP flux was weaker, it showed a transition from release to deposition with time, with the deposition flux gradually increasing in group T_2 and T_3 (Fig. 8d). In summary, results show that the nutrient changes in sediments and water were significantly affected by cyanobacteria, which was the main determining factor in nutrient flux and concentrations (Akagi and Zsolnay 2008; Brocke et al. 2015), Additionally, trends in cyanobacterial decomposition changed due to conditions such as DO, temperature, and the pH of water (Li et al. 2017), affecting the composition and activity of microorganisms, the porosity of sediments, and the accumulation of organic matter, further changing overall nutrient flux. Some previous studies have shown that pH and T in water can stimulate the release of dissolved nutrients from sediments (Xie et al. 2003). In addition, cyanobacterial decomposition induces the release of nutrients, organic matter, and water from sediments, resulting a concentration gradient at the water-sediment interface and generating flux (Denis et al. 2001). The decomposition of microorganisms can mineralize organic compounds in sediments and release polyphosphates, while converting insoluble P compounds into soluble ions, allowing their release into water (Jin et al. 2006). Results showed that the accumulation and decomposition of cyanobacteria caused OM and C_w to increase in surface sediment layers, while also influencing nutrient concentration gradients at the water-sediment interface, leading to nutrient flux.

Overall, the results of this study demonstrate that accumulation and decomposition of cyanobacteria exert a large influence on the form of nutrients in water. The spatial and temporal redistribution of nutrients in water and spatial nutrient concentration patterns are especially affected in the first 9 days of cyanobacterial decomposing. Therefore, the removal of cyanobacteria from the surface of waterbodies should be performed within 1 week of accumulation of cyanobacteria, which can effectively reduce the pollution induced by cyanobacterial decomposition.

4 Conclusions

Based on the results of quantitative simulation experiments, the following conclusions can be drawn: (1) Nutrients in water underwent a transition among different forms during cyanobacterial decomposition, with distinct changes in the physicochemical parameters (pH, DO, Ec, ORP, and UV_{254}) of water observed. This resulted in a simultaneous increase in C_w and OM in the surface sediment; (2) cyanobacteria and nutrients in water, as well as ΔOM and ΔC_w in surface sediments, exhibited good binomial relationships ($R^2 > 0.90$, $p < 0.05$); (3) the decomposition of cyanobacteria induces changes in nutrient concentrations in the surface layer of sediments, as shown by sediment surface enrichment at depths of 0–10 cm. As sediment depth increased, the response exhibited weak anti-interference and hysteresis; (4) the water-sediment interface flux of nutrients is related to the density of cyanobacteria, degradation time, and nutrient characteristics. In this study, the degree of flux was ranked in the descending order of TN > NH_4^+–N > NO_3^-–N > TP, with the deposition flux of TN in the T_3 group on day 20 reaching a maximum of 259.81 mg m^{-2} day^{-1}.

Laboratory tests do not fully replicate the on-site environmental conditions, omitting aspects, such as wind-induced waves, water currents, suspended matter content, plankton distribution, and other factors, which are difficult to control in the laboratory. Therefore, results of laboratory simulation experiments may be different from the field performance, which is a common problem in environmental research. However, this study provides some valuable reference information for further research on cyanobacterial decomposition.

Acknowledgments We thank our colleagues and students from Fudan University for helping with the measurements and Pengying Zhang for modifying the images. We also thank Mogoedit (http://www.mogoedit.com/) for its linguistic assistance during the preparation of this manuscript.

Funding information This study was financially supported by ABA Chemicals and the National Science and Technology Major Project (2017ZX07204005-04).

References

Aigars J (2001) Seasonal variations in phosphorus species in the surface sediments of the Gulf of Riga, Baltic Sea. Chemosphere 45:827–834

Akagi J, Zsolnay A (2008) Effects of long-term de-vegetation on the quantity and quality of water extractable organic matter (WEOM): biogeochemical implications. Chemosphere 72:1462–1466

Atkinson CA, Jolley DF, Simpson SL (2007) Effect of overlying water pH, dissolved oxygen, salinity and sediment disturbances on metal release and sequestration from metal contaminated marine sediments. Chemosphere 69:1428–1437

Bai X, Zhou Y (2012) The influence of tubificid worms bioturbation on organic phosphorus components and their vertical distribution in sediment of Lake Taihu. Acta Ecol Sin 32:5581–5588

Beversdorf LJ, Weirich CA, Bartlett SL, Miller TR (2017) Variable cyanobacterial toxin and metabolite profiles across six eutrophic lakes of differing physiochemical characteristics. Toxins 9:62–65

Bianchi TS (2000) Cyanobacterial blooms in the Baltic Sea: natural or human-induced? Limnol Oceanogr 45:716–726

Bjerring R, Sondergaard, Jeppesen (2013) Persistent internal phosphorus loading during summer in shallow;eutrophic lakes. Hydrobiologia 710:95–107

Brocke HJ, Polerecky L, De BD, Weber M, Claudet J, Nugues MM (2015) Organic matter degradation drives benthic cyanobacterial mat abundance on Caribbean coral reefs. PLoS One 10:1–19

Brodrick S, Cullen P, Maher W (1987) Determination of exchangeable inorganic nitrogen species in wetland soils. Bull Environ Contam Toxicol 38:377–378

Cao X, Wang Y, He J, Luo X, Zheng Z (2016) Phosphorus mobility among sediments, water and cyanobacteria enhanced by cyanobacteria blooms in eutrophic Lake Dianchi. Environ Pollut 219:580–582

Chen M, Cui J, Lin J, Ding S, Gong M, Ren M, Tsang D (2018a) Successful control of internal phosphorus loading after sediment dredging for 6 years: a field assessment using high-resolution sampling techniques. Sci Total Environ 927:616–617

Chen M, Ding S, Chen X, Sun Q, Fan X, Lin J, Ren M, Yang L, Zhang C (2018b) Mechanisms driving phosphorus release during algal blooms based on hourly changes in iron and phosphorus concentrations in sediments. Water Res 133:153–155

Chen X, Huang Y, Chen G, Li P, Shen Y, Davis TW (2018c) The secretion of organics by living Microcystis under the dark/anoxic condition and its enhancing effect on nitrate removal. Chemosphere 196:280–287

Cheng L, Shen Q, Zhou Q, Fan C, Shao S (2015) Precontrol of algae-induced black blooms through sediment dredging at appropriate depth in a typical eutrophic shallow lake. Ecol Eng 77:139–145

Christophoridis C, Fytianos K (2006) Conditions affecting the release of phosphorus from surface lake sediments. J Environ Qual 35:1181–1183

Chuai X, Wei D, Chen X, Wang X, Miao A, Xi B, He L, Yang L (2011) Phosphorus release from cyanobacterial blooms in Meiliang Bay of Lake Taihu, China. Ecol Eng 37:842–849

Cory RM, Kling GW (2018) Interactions between sunlight and microorganisms influence dissolved organic matter degradation along the aquatic continuum. Limnol Oceanogr Lett 3:102–116

Dai J, Chen D, Wu S, Wu X, Gao G, Tang X, Shao K, Lv X, Xue W, Yang Q (2018) Dynamics of phosphorus and bacterial phoX genes during the decomposition of Microcystis blooms in a mesocosm. PLoS One 13:1–20

Denis L, Grenz C, Alliot É, Rodier M (2001) Temporal variability in dissolved inorganic nitrogen fluxes at the sediment-water interface and related annual budget on a continental shelf (NW Mediterranean). Oceanol Acta 24:85–97

Ding S, Wang Y, Wang D, Li YY, Gong M, Zhang C (2016) In situ, high-resolution evidence for iron-coupled mobilization of phosphorus in sediments. Sci Rep 6:24341–24345

Ding S, Chen M, Gong M, Fan X, Qin B, Xu H, Gao SS, Jin Z, Tsang DCW, Zhang C (2018) Internal phosphorus loading from sediments causes seasonal nitrogen limitation for harmful algal blooms. Sci Total Environ 625:872–884

Duan HT, Ma RH, Xu XF, Kong FX, Zhang SX, Kong WJ, Hao JY, Shang LL (2012) Two-decade reconstruction of algal blooms in China's Lake Taihu. Environ Sci Technol 43:3522–3528

Forster S, Glud RN, Gundersen JK, Huettel M (1999) In situ study of bromide tracer and oxygen flux in coastal sediments. Estuar Coast Shelf Sci 49:813–827

Fujii M, Ono K, Yoshimura C, Miyamoto M (2018) The role of autochthonous organic matter in radioactive cesium accumulation to riverine fine sediments. Water Res 137:18–23

Gkelis S, Papadimitriou T, Zaoutsos N, Leonardos I (2014) Anthropogenic and climate-induced change favors toxic cyanobacteria blooms: evidence from monitoring a highly eutrophic, urban Mediterranean lake. Harmful Algae 39:322–333

Graham JL, Loftin KA, Meyer MT, Ziegler AC (2010) Cyanotoxin mixtures and taste-and-odor compounds in cyanobacterial blooms from the Midwestern United States. Environ Sci Technol 44:7361–7368

Grasso F, Michallet H, Barthélemy E (2011) Sediment transport associated with morphological beach changes forced by irregular asymmetric, skewed waves. J Geophys Res Oceans 3:116–119

Haas C, Gerke HH, Ellerbrock RH, Hallett PD, Horn R (2018) Relating soil organic matter composition to soil water repellency for soil biopore surfaces different in history from two Bt horizons of a Haplic Luvisol. Ecohydrology 11:1–11

Han L, Gao B, Hao H, Zhou H, Lu J, Sun K (2018) Lead contamination in sediments in the past 20 years: a challenge for China. Sci Total Environ 746:640–641

Henderson RK, Baker A, Parsons SA, Jefferson B (2008) Characterisation of algogenic organic matter extracted from cyanobacteria, green algae and diatoms. Water Res 42:3435–3445

Herrera-Silveira JA, Medina-Gomez I, Colli R (2002) Trophic status based on nutrient concentration scales and primary producers community of tropical coastal lagoons influenced by groundwater discharges. Hydrobiologia 475:91–98

Hoegh-Guldberg O, Mumby PJ, Hooten AJ, Steneck RS, Greenfield P, Gomez E, Harvell CD, Sale PF, Edwards AJ, Caldeira K (2009) Coral reefs under rapid climate change and ocean acidification. Science 318:1737–1742

House WA, Denison FH (2002) Exchange of inorganic phosphate between riverc waters and bed-sediments. Environ Sci Technol 36: 4295–4301

Hu J, Shen Q, Liu Y, Liu J (2007) Mobility of different phosphorus pools in the sediment of Lake Dianchi during cyanobacterial blooms. Environ Monit Assess 132:141–153

Iversen N, Bo BJ (1993) Diffusion coefficients of sulfate and methane in marine sediments: influence of porosity. Geochim Cosmochim Acta 57:571–578

Jiao F, Shi XR, Han FP, Yuan ZY (2016) Increasing aridity, temperature and soil pH induce soil C-N-P imbalance in grasslands. Sci Rep 6: 19601–19605

Jin X, Wang S, Pang Y, Chang FW (2006) Phosphorus fractions and the effect of pH on the phosphorus release of the sediments from different trophic areas in Taihu Lake, China. Environ Pollut 139:288–295

Kaiho K (1994) Benthic foraminiferal dissolved-oxygen index and dissolved-oxygen levels in the modern ocean. Geology 22:719–722

Keil RG, Hu FS, Tsamakis EC, Hedges JI (1994) Pollen in marine sediments as an indicator of oxidation of organic matter. Nature 369: 639–641

Kim TH, Kim G (2013) Factors controlling the C:N:P stoichiometry of dissolved organic matter in the N-limited, cyanobacteria-dominated East/Japan Sea. J Marine Syst 115(116):1–9

Kleeberg A, Kozerski HP (1997) Phosphorus release in Lake Großer Müggelsee and its implications for lake restoration. Hydrobiologia 342–343:9–26

Kuanyi L, Zhengwen L, Binhe G (2010) The fate of cyanobacterial blooms in vegetated and unvegetated sediments of a shallow eutrophic lake: a stable isotope tracer study. Water Res 44:1591–1597

Laskov C, Amelung W, Peiffer S (2002) Organic matter preservation in the sediment of an acidic mining lake. Environ Sci Technol 36: 4218–4221

Lavery PS, Oldham CE, Ghisalberti M (2010) The use of Fick's First Law for predicting porewater nutrient fluxes under diffusive conditions. Hydrol Process 15:2435–2451

Lei Z, Liao Q, Gu X, Wei H, Zhe Z, Fan C (2014) Oxygen and phosphorus dynamics in freshwater sediment after the deposition of flocculated cyanobacteria and the role of tubificid worms. J Hazard Mater 266:1–9

Li J, Yang X, Wang Z, Shan Y, Zheng Z (2015) Comparison of four aquatic plant treatment systems for nutrient removal from eutrophied water. Bioresour Technol 179:1–7

Li X, Chen H, Jiang X, Yu Z, Yao Q (2017) Impacts of human activities on nutrient transport in the Yellow River: the role of the water-sediment regulation scheme. Sci Total Environ 592:161–170

Maagd GJD, Hendriks AJ, Seinen W, Sijm DTHM (1999) pH-dependent hydrophobicity of the cyanobacteria toxin microcystin-LR. Water Res 33:677–680

Masscheleyn PH, Delaune RD, Jr WHP (1990) Transformations of selenium as affected by sediment oxidation-reduction potential and pH. Environ Sci Technol 24:91–96

Matisoff G, Watson SB, Guo J, Duewiger A, Steely R (2017) Sediment and nutrient distribution and resuspension in Lake Winnipeg. Sci Total Environ 575:173–186

Mccabe AJ, Arnold WA (2017) Reactivity of triplet excited states of dissolved natural organic matter in stormflow from mixed-use watersheds. Environ Sci Technol 51:1–9

Mukherjee B, Nivedita M, Mukherjee D (2014) Modelling system dynamics and phytoplankton diversity at Ranchi lake using the carbon and nutrient mass balance equations. J Environ Biol 35:577–581

Murphy KR, Butler KD, Spencer RGM, Stedmon CA, Boehme JR, Aiken GR (2010) Measurement of dissolved organic matter fluorescence in aquatic environments: an interlaboratory comparison. Environ Sci Technol 44:9405–9412

Nikolai SJ, Dzialowski AR (2014) Effects of internal phosphorus loading on nutrient limitation in a eutrophic reservoir. Limnologica 49:33–41

Papadimitriou T, Katsiapi M, Vlachopoulos K, Christopoulos A, Laspidou C, Moustaka-Gouni M, Kormas K (2018) Cyanotoxins as the "common suspects" for the Dalmatian pelican (Pelecanus crispus) deaths in a Mediterranean reconstructed reservoir. Environ Pollut 234:779–787

Paytan A, Roberts K, Watson S, Peek S, Chuang PC, Defforey D, Kendall C (2016) Internal loading of phosphate in Lake Erie Central Basin. Sci Total Environ 579:1356–1361

Qin B, Zhu G, Gao G, Zhang Y, Li W, Paerl HW, Carmichael WW (2010) A drinking water crisis in Lake Taihu, China: linkage to climatic variability and lake management. Environ Manag 45:105–112

Qinglong WU, Xie P, Yang L, Gao G, Liu Z, Pan G, Zhu B (2008) Ecological consequences of cyanobacetrial blooms in lakes and their countermeasures. Adv Earth Sci 23:1115–1123

Queiroz MI, Lopes EJ, Zepka LQ, Bastos RG, Goldbeck R (2007) The kinetics of the removal of nitrogen and organic matter from parboiled rice effluent by cyanobacteria in a stirred batch reactor. Bioresour Technol 98:2163–2169

Ram A, Borole DV, Rokade MA, Zingde MD (2009) Diagenesis and bioavailability of mercury in the contaminated sediments of Ulhas Estuary, India. Mar Pollut Bull 58:1685–1693

Ruban V, López-Sánchez JF, Pardo P, Rauret G, Muntau H, Quevauviller P (2001) Harmonized protocol and certified reference material for the determination of extractable contents of phosphorus in freshwater sediments-a synthesis of recent works. Fresenius J Anal Chem 370:224–228

Russo D, Siciliano A, Guida M, Andreozzi R, Reis NM, Li GP, Marotta R (2018) Removal of antiretroviral drugs stavudine and zidovudine in water under UV_{254} and UV_{254}/H_2O_2 processes: quantum yields, kinetics and ecotoxicology assessment. J Hazard Mater 349:195–204

Sahlsten E, Sörensson F (1989) Planktonic nitrogen transformations during a declining cyanobacteria bloom in the Baltic Sea. J Plankton Res 11:1117–1128

Seelen EA, Massey GM, Mason RP (2018) Role of sediment resuspension on estuarine suspended particulate mercury dynamics. Environ Sci Technol 52:7736–7744

Shi L, Huang Y, Zhang M, Yu Y, Lu Y, Kong F (2017) Bacterial community dynamics and functional variation during the long-term decomposition of cyanobacterial blooms in-vitro. Sci Total Environ 598:77–86

Shiraishi F, Hanzawa Y, Okumura T, Tomioka N, Yu K, Suga H, Takahashi Y, Kano A (2017) Cyanobacterial exopolymer properties differentiate microbial carbonate fabrics. Sci Rep 7:11805–11809

Stone M, English MC (1993) Geochemical composition, phosphorus speciation and mass transport of fine-grained sediment in two Lake Erie tributaries. Hydrobiologia 253:17–29

Su M, Jia D, Yu J, Vogt RD, Wang J, An W, Yang M (2017) Reducing production of taste and odor by deep-living cyanobacteria in drinking water reservoirs by regulation of water level. Sci Total Environ 574:1477–1483

Tisdall JM, Oades JM (2010) Organic matter and water-stable aggregates in soils. Eur J Soil Sci 33:141–163

Trimmer M, Nicholls JC, Deflandre B (2003) Anaerobic ammonium oxidation measured in sediments along the Thames estuary, United Kingdom. Appl Environ Microbiol 69:6447–6454

Wert EC, Rosarioortiz FL (2013) Intracellular organic matter from cyanobacteria as a precursor for carbonaceous and nitrogenous disinfection byproducts. Environ Sci Technol 47:6332–6340

Wieland A, Kühl M, Mcgowan L, Fourçans A, Duran R, Caumette P, Oteyza TGD, Grimalt JO, Solé A, Diestra E (2003) Microbial mats on the Orkney Islands revisited: microenvironment and microbial community composition. Microb Ecol 46:371–390

Wu S, He S, Huang J, Gu J, Zhou W, Lei G (2017) Decomposition of emergent aquatic plant (cattail) litter under different conditions and the influence on water quality. Water Air Soil Pollut 228:70–75

Xie LQ, Xie P, Tang HJ (2003) Enhancement of dissolved phosphorus release from sediment to lake water by Microcystis blooms-an enclosure experiment in a hyper-eutrophic, subtropical Chinese lake. Environ Pollut 122:391–399

Xie Y, Yu D, Ren B (2004) Effects of nitrogen and phosphorus availability on the decomposition of aquatic plants. Aquat Bot 80:1–37

Xu H, Zhu G, Qin B, Paerl HW (2013) Growth response of Microcystis spp. to iron enrichment in different;regions of Lake Taihu, China. Hydrobiologia 700:187–202

Yan B, Liu Z, Huang R, Xu Y, Liu D, Lin TF, Cui F (2017) Optimization of the determination method for dissolved cyanobacterial toxin BMAA in natural water. Anal Chem 89:10991–10998

Yang L, Choi JH, Jin H (2014) Benthic flux of dissolved organic matter from lake sediment at different redox conditions and the possible effects of biogeochemical processes. Water Res 61:97–107

Yang Y, Gao B, Hao H, Zhou H, Lu J (2017) Nitrogen and phosphorus in sediments in China: a national-scale assessment and review. Sci Total Environ 576:840–849

Ye W, Liu X, Lin S, Tan J, Pan J, Li D, Yang H (2010) The vertical distribution of bacterial and archaeal communities in the water and sediment of Lake Taihu. FEMS Microbiol Ecol 70:107–120

Ye Y, Chang PH, Hartert J, Wigginton KR (2018) Reactivity of enveloped virus genome, proteins, and lipids with free chlorine and UV_{254}. Environ Sci Technol 52:7698–7708

Yu J, Zhong J, Chen Q, Huang W, Hu L, Zhang Y, Fan C (2018) An investigation of the effects of capping on internal phosphorus release from sediments under rooted macrophytes (Phragmites australis) revegetation. Environ Sci Pollut Res 25:24682–24694

Zastepa A, Pick FR, Blais JM (2017) Distribution and flux of microcystin congeners in lake sediments. Lake Reserv Manage 33:444–451

Zhang B, Zhu C, Jia Y, Zhang X, Dai X, Shen Z, Jiang J, Wang X (2017) Surface sediment density and moisture content in north slope of South China Sea. Acta Geol Sin 91:155–156